PLASTIC ZONE EVOLUTION IN NOTCHED BARS: IMPLICATIONS IN ENVIRONMENTALLY-ASSISTED FRACTURE

J. TORIBIO

Department of Engineering, University of La Coruña
E.T.S.I. Caminos, Pol. Sabón, P. 12-14, 15141 Arteixo, La Coruña, Spain

ABSTRACT

This article deals with the evolution of the plastic zone in notched bars as a function of the constitutive equation of the material and the geometry of the notch, with special emphasis on its implications in environmentally assisted fracture (EAF) of metallic specimens with such kind of geometry. The analysis is focussed, firstly, on the evolution of the local strain rate at the notch tip, whose role in environmentally-induced fracture processes is determining, and secondly, on the comparison between the plastic zone size and the hydrogen affected region in hydrogen embrittlement tests, which clarifies the hydrogen transport mechanism.

KEYWORDS

Notched bar, plastic zone evolution, environmentally assisted fracture, hydrogen embrittlement, local strain rate, hydrogen affected region.

INTRODUCTION

Environmentally-assisted fracture (EAF) always involves a transient or time-dependent process, either dissolution of material produced by the environment, or embrittlement due to hydrogen created by chemical reactions. In any case, there is a balance between the action of the aggressive environment and the time, which determines the severity of the process (Scully, 1980; Ford, 1982). In this context, plastic zone evolution —which is itself also a transient or time-dependent phenomenon— has fundamental importance in controlling and influencing the EAF process.

For fracture phenomena which promote metal dissolution (anodic regime of EAF), failure load increases or decreases as the displacement rate increases, because there is a balance between the creation and rupture of the oxide film on the sample surface (Parkins, 1979). For hydrogen embrittlement phenomena, in which there is no metal dissolution (cathodic regime of EAF), failure load is always an increasing function of the displacement rate, since the slower the loading process, the more the hydrogen diffusion into the sample (Scully and Moran, 1988).

However, the *displacement rate* is not the variable actually representative, and it only allows the establishment of qualitative phenomenological relations. To obtain quantitative relations and compare results from different EAF tests, it is necessary to calculate the *local strain rate* at the crack or notch tip, because at that point the environmental attack is localized and crack (or

notch) tip strain rate controls the environmental cracking process (Rieck *et al.*, 1989). The only previous research about this matter refers to the computation of (local) strain rate at a crack tip (Lidbury, 1983; Maiya, 1987; Andresen and Ford; 1988; Parkins, 1990). An inherent limitation of all these expressions for local strain rate at the crack tip is that they do not take into account the constitutive equation of the material and the spreading of the plastic zone, which clearly influences the value of local strain rate, as is demonstrated in the present paper.

In the case of hydrogen embrittlement, the interactions between hydrogen and plasticity are now well known (Hirth, 1980), and two main types of hydrogen transport in metals have been proposed: *lattice diffusion* (Johnson *et al.*, 1958; Troiano, 1960) and *dislocation sweeping* (Tien *et al.*, 1976; Johnson and Hirth, 1976). There is a strong controversy about the main mechanism of hydrogen transport in steel and whether or not dislocation sweeping can be considered an embrittlement mechanism per se.

This paper is focussed on the spreading of the plastic zone in notched bars, as a function of the constitutive equation of the material and the geometry of the notch. An analysis is made of the influence of plasticity development on the evolution of local strain rate at the notch tip, which is the relevant variable in EAF processes of any type (anodic dissolution or hydrogen embrittlement). Regarding specifically hydrogen assisted fracture, the evolution of the plastic zone allows the establisment of conclusions on the interactions between hydrogen and dislocations and on the main hydrogen transport mechanism.

PLASTIC ZONE EVOLUTION

The material model used in the computations corresponds to the real high strength steel used in the experimental programme, whose stress-strain curve can be represented by the following Ramberg-Osgood equation:

$$\varepsilon = \sigma/199000 + (\sigma/2100)^{4.9}\ , \quad \sigma \text{ in MPa} \tag{1}$$

Four axisymmetric notched geometries of maximum and minimum notch depths and radii were chosen (Fig.1), with a diameter D=11.25 mm.

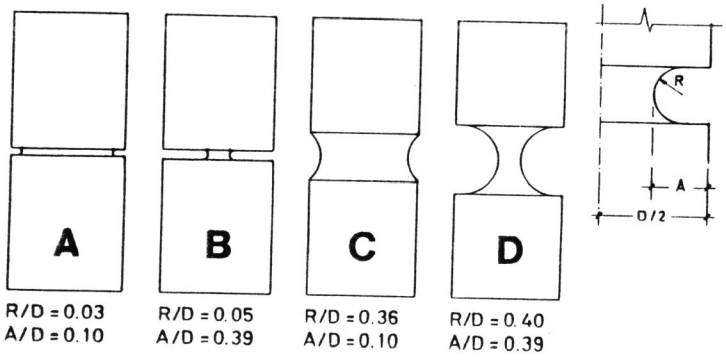

Fig. 1. Notched geometries (R: notch radius, A: notch depth, D: sample diameter).

To analyze the evolution of the plastic zone, the yielding criterion used in the numerical computations was that of Von Mises:

$$\bar{\sigma} = \sigma_Y \tag{2}$$

where $\bar{\sigma}$ is the effective or equivalent stress and $\sigma_Y = \sigma_{0.1} = 500$MPa, yield strength measured at 0.1% of strain. Properly speaking, it is the limit of material linear behaviour. According to this criterion, the boundaries of the progressive plastic zones for different values of the global displacement u_G appear in Fig.2, where u_G represents the displacement between sample ends (L and D are the length and diameter of the sample, respectively). Curves correspond to different values of the dimensionless parameter u_G/D (L/D=4) and therefore they reflect the progressive spreading of the plastic zone as the external load applied on the sample —external displacement— increases. In all cases, computation was extended until the situation corresponding to the fracture of the specimen in the test performed in air (see experimental section).

Fig. 2 shows that plastic deformation always initiates at the notch tip and spreads towards the inner part until the whole net section is under plastic regime, this result being general for all geometries analyzed. Considering the shape of the plastic zone, two considerations may be made:

(i) Geometry A presents a plastic zone which starts from the notch tip and branches as it approaches to the sample axis. Its mechanical behaviour is similar to that of a plastic hinge, opening in the vicinity of the notch tip and keeping stiff the rest of net section.

(ii) The spreading of the plastic zone is global in geometries A and C (plastic zone covers an important part of the sample), whereas it is localized in geometries B and D (plastic zone is restricted to the sample neck).

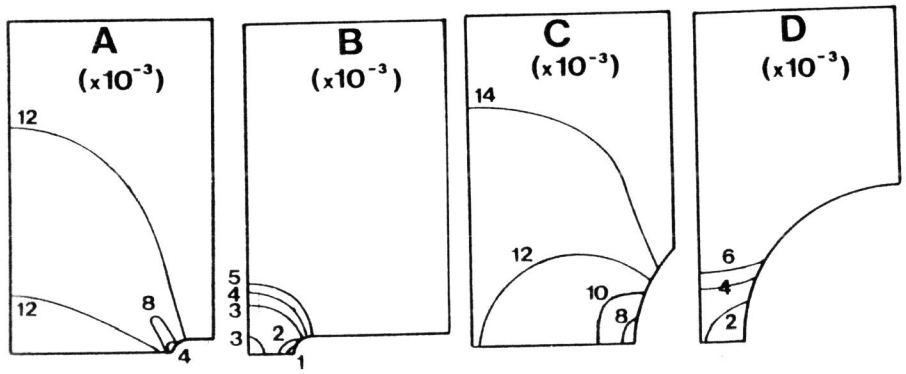

Fig. 2. Spreading of the plastic zone, for different values of u_G/D, where u_G is the global displacement applied to the sample ends (L=4D) and D the sample diameter.

EFFECT OF PLASTIC ZONE ON LOCAL STRAIN RATE

In this section local and global strain rates are defined, the former being the variable which governs the EAF process, and the latter being the variable which can be controlled by the testing machine when notched specimens are tested in a corrosive medium.

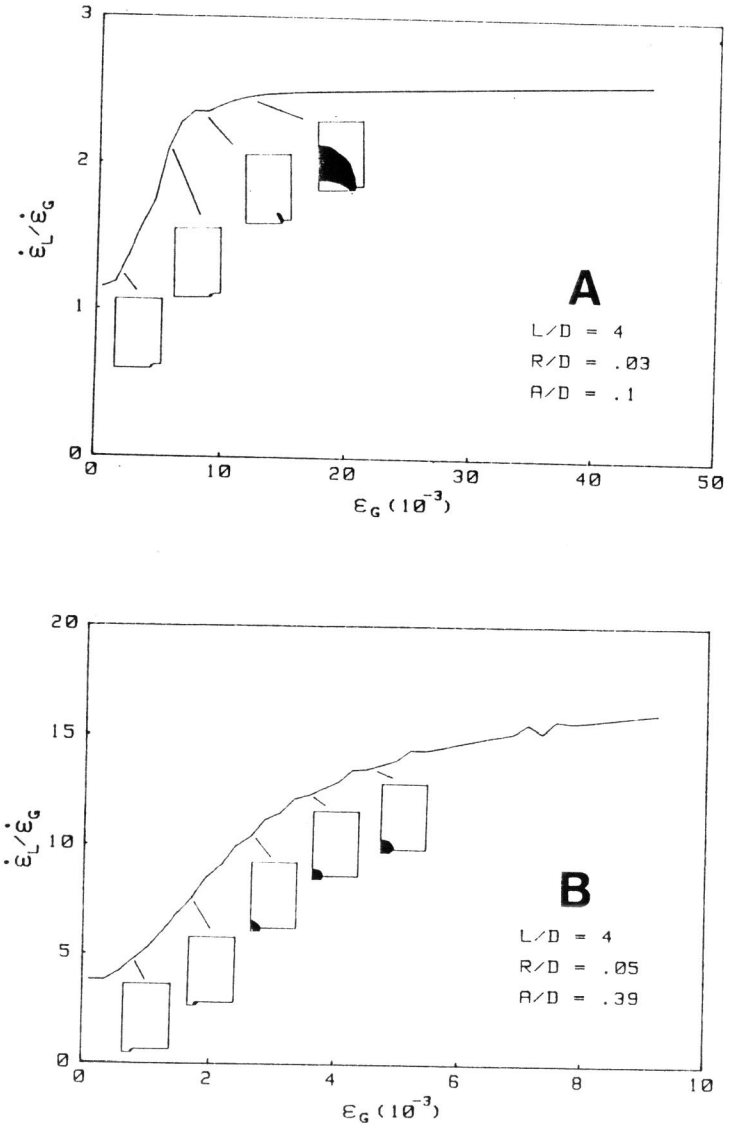

Fig. 3. Relationship between local and global strain rates and evolution of the plastic zone (geometries A and B).

Local strain ε_L is defined as the strain associated with a local reference length L_L (small enough to guarantee the convergence) parallel to the bar axis and placed at the notch tip, i.e:

$$\varepsilon_L = \Delta L_L / L_L \tag{3}$$

Global strain ε_G is defined as the relative displacement between the ends of a sample of length L (global displacement u_G), divided by a characteristic length of the geometry (diameter D) to obtain a dimensionless variable:

$$\varepsilon_G = u_G / D \tag{4}$$

It must be noticed that global strain is a dimensionless displacement and, contrarily to local strain, it is not a strain in the Continuum Mechanics sense, since the strain is non uniform along the axial direction in a notched geometry. Strictly speaking, therefore, it should be called *dimensionless global displacement.*

Local and global strain rates can be obtained on time-derivation of expressions (3) and (4).

$$\dot{\varepsilon}_L = (\Delta L_L^{i+1} - \Delta L_L^{i}) / L_L / \Delta t \tag{5}$$

$$\dot{\varepsilon}_G = (u_G^{i+1} - u_G^{i}) / D / \Delta t \tag{6}$$

where superscripts i and i+1 mean a loading step and the next one. The value Δt represents the time interval between two loading steps, which can be constant or variable from one to another step. From considerations of convergence, the chosen values for local and global reference lengths are L_L=0.01D and L=4D, respectively.

In Fig. 3, a plot is given of the relationship between local and global strain rates as a function of global strain (for geometries A and B). Evolution of plastic zone is also presented (shaded area). Relationship between local and global strain rates changes with the time, as the plastic zone spreads or the global strain (or more properly global displacement) increases. For all geometries analyzed in this paper the curve has always the same general aspect, an three regions can be distinguished, each of them representing a phase of the process:

(i) Region I (*Elastic phase*): Horizontal. The whole sample is under elastic regime. The relationship between local and global strain rate is constant or, in other words, a constant externally applied global strain rate produces a constant local strain rate at the notch tip. In this case the elastic phase only represents a small percentage of the whole loading process. Length of elastic region is a function of yield strength of the material, increasing with it.

(ii) Region II (*Transition phase*): Big slope. Plastic deformation starts at notch tip and spreads progressively towards the inner region. The shape of the plastic zone depends on the particular geometry, while its size increases as global strain rate increases.

(iii) Region III (*Plastic phase*): Slightly increasing or quasi-horizontal. Plastic zone reaches the sample axis. In this case the relationship between local and global strain rate is more or less constant, but there is a clear magnification of local strain rate of the notch tip due to the fact that all net section is under plastic regime.

The above facts demonstrate the effect of the spreading of the plastic zone on the evolution of local strain rate at the notch tip, which is the relevant variable in EAF processes on notched specimens, as demonstrated in previous works (Toribio and Elices, 1992).

EFFECT OF PLASTIC ZONE ON HYDROGEN TRANSPORT

This section tries to establish experimental bases to clarify the main mechanism of hydrogen transport in pearlitic steels, by relating the spreading of the plastic zone with the hydrogen affected region in hydrogen embrittlement processes. The analysis is based on the existence of a non conventional microscopic fracture mode, the *Tearing Topography Surface (T.T.S.)*, associated with hydrogen embrittlement phenomena in this kind of steel (Toribio *et. al*, 1991), whose fractographic appearance is given in Fig. 4.

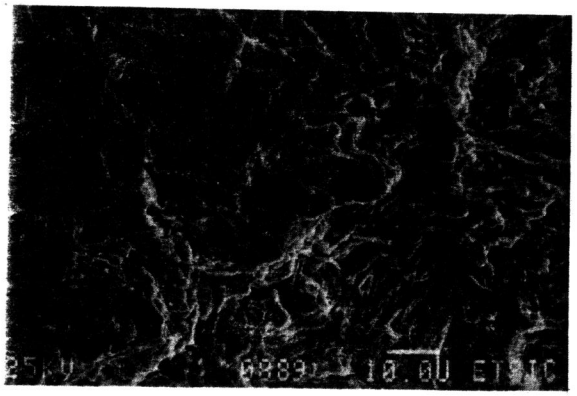

Fig. 4 Tearing Topography Surface.

The correlation between the Tearing Topography Surface and hydrogen effects gives an approach to clarifying which is the main mechanism of hydrogen transport. The TTS size has to be compared with the distribution of hydrostatic stress in the sample, or with the extension of the plastic zone, depending on the mechanism of hydrogen transport under consideration. If lattice diffusion were the predominant mechanism, then the hydrostatic stress would be an outstanding variable. On the other hand, if hydrogen were mainly transported by dislocation sweeping, then the evolution and size of the plastic zone would be relevant , since outside that zone there is no movement of dislocations.

The elastic-plastic FEM analysis demonstrated that the hydrostatic stress levels changed with the loading process, but the point of maximum hydrostatic stress always remains at depth x_S (characteristic of the geometry) from the notch tip, as demonstrated by Toribio *et al.* (1991). The geometry B (maximum depth, minimum radius) presents special advantages for the analysis of hydrogen transport, since the point of maximum hydrostatic stress is located at the center of the net section in this case, and therefore hydrogen is atracted to that point, thus producing a broader affected region detectable by fractographic analysis, while at the same time providing a plastic zone small enough to restrict the movement of dislocations to a reduced area. The probability of detecting hydrogen effects outside the plastic zone is high.

For the experimental programme, a commercial hot rolled pearlitic steel –whose stress-strain curve can be modelled according to the Ramberg-Osgood expression (1)– was used, machined with the four geometries analyzed in previous sections. Slow strain rate tests (SSRT) were performed in an aqueous solution of 1 g/l calcium hydroxide plus 0.1 g/l sodium chloride, with a pH of 12.5, at a constant potential of -1200mV SCE, corresponding to hydrogen embrittlement conditions (Toribio *et al.*, 1991). A broad range of displacement rates (between 10^{-10} and 10^{-7}m/s) was covered in the SSRT to evaluate different degrees of hydrogen damage. For comparison purposes, two fracture tests of each geometry were performed in air.

Table 1. Evolution of the plastic zone and hydrogen affected area

$\dot{u}$ (m/s)	t_c (s)	x_{TTS} (mm)	x_{PZ} (mm)
1.00×10^{-7}	720	0.10	NET SECTION
1.03×10^{-7}	780	0.15	NET SECTION
1.02×10^{-8}	5760	0.25	NET SECTION
8.70×10^{-9}	7380	0.21	NET SECTION
6.90×10^{-9}	8520	0.27	NET SECTION
6.23×10^{-9}	11160	0.30	NET SECTION
6.02×10^{-10}	75600	0.60	NET SECTION
1.87×10^{-10}	143040	0.93	0.33
1.12×10^{-10}	262800	1.00	0.41

$\dot{u}$: displacement rate; t_c: time to failure or critical time;
x_{TTS}: depth of the TTS region or hydrogen affected area;
x_{PZ}: depth of the plastic zone at the end of each test.

Table 1 gives the experimental results of the SSRT for the geometry B. In the majority of cases, the plastic zone (PZ) clearly exceeds the hydrogen affected region (TTS) and does not have any relation with it, which is consistent with previous results for very different notched geometries (Toribio et al., 1991). This experimental fact does not prove anything about the hydrogen transport by dislocation sweeping, since the TTS region is completely surrounded by the plastic zone where dislocations move. It only proves that there is no net balance of hydrogen transport in the whole extension of the plastic zone. Nevertheless, for the geometry B (R/D=0.05, A/D=0.39) and for the two slowest tests, the situation is inverse; in this case the hydrogen affected area (TTS) exceeds the only region in which there is dislocation movement, and the hydrogen transport cannot be attributed to dislocation dragging, but only to a random-walk diffusion. It is not, however, conventional diffusion according to classical Fick's laws, but stress-assisted diffusion in which the hydrostatic stress field plays a very important role in accelerating the diffusion and enlarging the penetration distance. It is significant that the depth of the TTS region in the slowest test (quasi-static) almost reaches the point of maximum hydrostatic stress, a general result for all geometries (Toribio et. al, 1991). For the particular geometry described here, this point is exactly at the centre of the sample.

CONCLUSIONS

1. Plastic zone spreading in the vicinity of notch tips with different geometries was numerically computed up to the fracture instant in air environment. Yielding is global in geometries A and C, whereas it is a more localized phenomenon in geometries B and D.

2. Local strain rate at the notch tip —relevant variable in EAF processes— depends not only on the notch geometry and the loading process, but also on the spreading of the plastic zone and thus on the load externally applied on the sample.

3. In some cases the hydrogen affected region (TTS) exceeds the plastic zone size, which provides experimental evidence of a hydrogen transport mechanism by stress-assisted random-walk diffusion in this pearlitic steel.

Acknowledgments

This work was supported by the Spanish Office for Science and Technological Research (CICYT), under Grant MAT91–0113–CE. The author would like to thank Professor M. Elices, head of the Material Science Department of the Polytechnical University of Madrid, for his encouragement and assistance, to Dr. A.M. Lancha, CIEMAT, Spain, for the SEM fractographic analysis, and to Mr. J. Monar, *Nueva Montaña Quijano Co.*, Santander, Spain, for providing the steel used in the experimental programme. In addition, the author wishes to express his gratitude to the *Colegio de Ingenieros de Caminos, Canales y Puertos–Demarcación de Galicia*, Spain, for the financial support of technical trips during the final stages of this work.

REFERENCES

Andresen, P.L. and Ford, F.P.(1988) 'Life prediction by mechanistic modeling and system monitoring of environmental cracking of iron and nickel alloys in aqueous systems', *Mater. Sci. Engng.* **A103**, 167-184.

Ford, F.P. (1982) 'Stress corrosion cracking', in *Corrosion Processes* (Parkins, R.N., Ed.) pp. 271-309, Applied Science Publishers, London.

Hirth, J.P. (1980) 'Effects of hydrogen on the properties of iron and steel', *Metall. Trans.* **11A**, 861-890.

Johnson, H.H. and Hirth, J.P. (1976) 'Internal hydrogen supersaturation produced by dislocation transport', *Metall. Trans.* **7A**, 1543-1548.

Johnson, H.H., Morlet, J.G. and Troiano, A.R. (1958) 'Hydrogen, crack initiation, and delayed failure in steel', *Trans. Met. Soc. AIME* **212**, 528-536.

Lidbury, D.P.G. (1983) 'The estimation of crack tip strain rate parameters characterizing environment assisted crack growth data', in *Embrittlement by the Localized Crack Environment*, pp. 149-172 (R.P. Gangloff, Ed.). AIME, New York.

Maiya, P.S.(1987) 'Prediction of environmental and strain-rate effects on the stress corrosion cracking of austenitic stainless steels', *J.Pressure Vessel Tech.* **109**, 116-123.

Parkins, R.N. (1979) 'Development of strain-rate testing and its implications', in *Stress Corrosion Cracking - The Slow Strain Rate Technique, ASTM STP 665* (Ugiansky, G.M. and Payer, J.H., Eds.) pp. 5-25, ASTM, Philadelphia.

Parkins, R.N. (1990) 'Strain rate effects in stress corrosion cracking', *Corrosion* **46**, 178-189.

Rieck, R.M. , Atrens, A. and Smith, I.O. (1989) 'The role of crack tip strain rate in the stress corrosion cracking of high strength steels in water', *Metall. Trans.* **20A**, 889-895.

Scully, J.C. (1980) 'The interaction of strain-rate and repassivation rate in stress corrosion crack propagation', *Corros. Sci.* **20**, 997-1016.

Scully, J.R. and Moran, P.J. (1988) 'Influence of strain on the environmental hydrogen-assisted cracking of a high-strength steel in sodium chloride solution', *Corrosion* **44**, 176-185.

Tien, J.K., Thompson, A.W., Bernstein, I.M. and Richards, R.J. (1976) 'Hydrogen transport by dislocations', *Metall. Trans.* **7A**, 821-829.

Toribio, J. and Elices, M. (1992) 'The Role of Local Strain Rate in the Hydrogen Embrittlement of Round-Notched Samples´, *Corros. Sci.* (In press).

Toribio, J., Lancha, A.M. and Elices, M. (1991) 'Macroscopic Variables Governing the Microscopic Fracture of Pearlitic Steels' *Mater. Sci. Engng.* **A 145**, 167-177.

Troiano, A.R. (1960) 'The role of hydrogen and other interstitials in the mechanical behavior of metals', *Trans. ASM* **52**, 54-80.